Current drive by high intensity, pulsed, electron cyclotron wave packets

Abhay K. Ram[1,*], *Kyriakos* Hizanidis[2,**], and *Richard J.* Temkin[1,***]

[1]Plasma Science and Fusion Center, Massachusetts Institute of Technology, Cambridge, MA 02139. USA.
[2]National Technical University of Athens, 157 73 Zographou, Greece.

Abstract. The nonlinear interaction of electrons with a high intensity, spatially localized, Gaussian, electromagnetic wave packet, or beam, in the electron cyclotron range of frequencies is described by the relativistic Lorentz equation. There are two distinct sets of electrons that result from wave-particle interactions. One set of electrons is reflected by the ponderomotive force due to the spatial variation of the wave packet. The second set of electrons are energetic enough to traverse across the wave packet. Both sets of electrons can exchange energy and momentum with the wave packet. The trapping of electrons in plane waves, which are constituents of the Gaussian beam, leads to dynamics that is distinctly different from quasilinear modeling of wave-particle interactions. This paper illustrates the changes that occur in the electron motion as a result of the nonlinear interaction. The dynamical differences between electrons interacting with a wave packet composed of ordinary electromagnetic waves and electrons interacting with a wave packet composed of extraordinary waves are exemplified.

1 Introduction

In the early 1990s, high power, pulsed, microwaves, in the electron cyclotron (EC) frequency range, were used in the Microwave Tokamak Experiment (MTX) [1] for heating and for current generation in high density plasmas. Bursts of pulses were generated by a free-electron laser at a frequency of 140 GHz with powers up to 2 GW, and pulse durations of 20-30 ns. It was noted in [1] that "extrapolation to reactor heating and current drive predicts high efficiency." In the intervening years, significant advances have occurred in the technology of high power millimeter wave sources. Gyrotrons now routinely achieve megawatt power levels in continuous wave operations – 140 GHz for W7-X and 170 GHz for ITER. Relativistic gyrotrons can operate in a pulsed mode, in the millimeter wavelength range, at power levels ranging from 10 to 100 MW [2]. These developments have led to our studies on the interaction of electrons with high peak power EC fields, while, simultaneously, aiming to optimize current drive in fusion plasmas.

The nonlinear interaction of electrons with high intensity wave packets in the EC frequency range is described by the relativistic Lorentz equation. The wave packet is spatially localized perpendicular to its direction of propagation. We find that the interaction of electrons with an extraordinary EC wave is very different from the interaction with an ordinary wave. Consequently, the polarization of the EC beam has an important effect in the wave-particle interaction. The components of the electron momentum, along and across the magnetic field, are a function of the wave power and the direction of wave propagation. The interaction of electrons with a wave packet is significantly different from that with a large amplitude plane wave [3]. The interaction with a spatially confined wave packet leads to a wider variety of nonlinear phenomena including spatial modifications to the temperature profile as well as affecting MHD activity. Recently, a study of the nonlinear interaction of electrons with a Gaussian beam, in a low temperature plasma, has concluded that EC waves could be used in the pre-ionization phase for start-up of tokamak operations [4]. The theoretical and computational studies show that the nonlinear interaction with the beam provides sufficient energy to electrons so as to ionize the plasma.

In the usual quasilinear theory, the electron motion is given by linear theory which ignores any nonlinear effects, for example, due to trapping or the ponderomotive force. The limitations of quasilinear theory and its applicability to even the present-day EC heated plasmas has been questioned [5, 6]. The reason being that trapping of electrons in waves cannot be neglected or ignored. Our studies show that electrons interacting with EC beams do not follow linear orbits – a bedrock of quasilinear theory. In addition, our calculations lend credence to the claims made in [1], that high powered EC waves will lead to efficient heating and current drive in fusion plasmas through nonlinear effects. The theoretical studies of wave-particle interactions discussed in this paper, along with the advances in the technology of high peak power sources, may offer a breakthrough in achieving steady-state operations in reactor scale plasmas.

*e-mail: abhay@mit.edu
**e-mail: kyriakos@central.ntua.gr
***e-mail: temkin@psfc.mit.edu

2 Description of the Gaussian beam

The EC Gaussian wave packet is assumed to be a superposition of plane waves having the same angular frequency ω_0. Each plane wave satisfies the local plasma dispersion relation and its polarization is obtained by using the cold plasma permittivity in Maxwell's equations. Among the set of plane waves, consider the one with the maximum amplitude of the Poynting flux. Let $\mathbf{k}_0$ is the wave vector of this particular plane wave and $\hat{\mathbf{s}}_0$ be the unit vector along the direction of the group velocity; $\hat{\mathbf{s}}_0$ essentially determines the axis of the beam. The time-averaged Poynting flux of the Gaussian beam is given by,

$$\langle \mathbf{S} \rangle \;=\; \frac{P_0}{\pi w^2}\; \exp\left(-\frac{|\mathbf{r}_{0\perp}|^2}{w^2}\right)\; \hat{\mathbf{s}}_0. \qquad (1)$$

Here P_0 is the total power flowing along the beam, $w/\sqrt{2}$ is the beam radius normal to $\hat{\mathbf{s}}_0$, and $\mathbf{r}_{0\perp}$ is the position vector transverse to the beam – the beam axis being at $\mathbf{r}_{0\perp} = 0$.

The electric field associated with the Gaussian beam is derived from the time-averaged Poynting flux of each associated planar wave. After some algebraic manipulations, we obtain the following expression for the electric field at position $\mathbf{r}$ and time t,

$$\mathbf{E}_{RF}\,(\mathbf{r},t) \;=\; E_0\,\mathrm{Re}\left[e^{-i\omega_0 t}\;\frac{1}{N}\;\sum_{\mathbf{n}}\;E_n\;\tilde{\mathbf{e}}_n \exp\left(i\mathbf{k}.\mathbf{r}\right)\right], \quad (2)$$

where Re indicates the real part of the expression inclosed within the brackets, and N is the total number of plane waves included in the representation of the Gaussian beam. The summation is over the normalized wave vectors $\mathbf{n} = c\mathbf{k}/\omega_0$ where c is the speed of light. In the Cartesian coordinate system $\mathbf{n} = \left(n_x, n_y, n_z\right)$ with the z direction being along the magnetic field and x being the direction of the plasma inhomogeneity. It is important to realize that the summation is actually a double sum – the components of $\mathbf{n}$ are not all independent since each plane wave satisfies the cold plasma dispersion relation. In Eq. 2, $\tilde{\mathbf{e}}_n$ is the electric field polarization, normalized to a unit norm, of the n-th plane wave, and

$$E_n \;=\; e^{\left(-w^2\,|\mathbf{k}-\mathbf{k}_0|^2\,/2\right)}. \qquad (3)$$

where $\mathbf{n}_0 = c\mathbf{k}_0/\omega_0$. The amplitude E_0 is,

$$E_0 \;=\; \sqrt{\frac{2P_0}{\pi w^2}}\;\left(\frac{\mu_0}{\epsilon_0}\right)^{1/4}\;S \qquad (4)$$

where ϵ_0 and μ_0 are the free space permittivity and permeability, respectively, and

$$S \;=\; \left(\frac{1}{\pi}\;\frac{w^2\Delta k_x^S\,\Delta k_y^S}{\mathrm{Re}\left\{\hat{\mathbf{s}}_0.\mathbf{n}_0 - (\hat{\mathbf{s}}_0.\tilde{\mathbf{e}}_n)\,(\tilde{\mathbf{e}}_n^*.\mathbf{n}_0)\right\}\;C_N}\right)^{1/2}, \qquad (5)$$

and,

$$C_N \;=\; \frac{1}{N}\;\sum_n \exp\left[\frac{w^2}{2}\;\left\{(\mathbf{k}-\mathbf{k}_0)\,.\mathbf{k}_\perp^S - |\mathbf{k}-\mathbf{k}_0|^2\right\}\right]. \qquad (6)$$

In Eqs. 5 and 6, k_x^s, k_y^s, and $\mathbf{k}_\perp^s$ are defined with respect to $\hat{\mathbf{s}}_0$. If we define the unit vectors in the Cartesian coordinate system with respect to the beam as $\left(\hat{\mathbf{x}}^S, \hat{\mathbf{y}}^S, \hat{\mathbf{s}}_0\right)$, then k_x^s and k_y^s are components of $\mathbf{k}$ along $\hat{\mathbf{x}}^S$ and $\hat{\mathbf{y}}^S$, respectively. Correspondingly, for the Gaussian beam, Δk_x^S and Δk_y^S are the spreads in the wave vectors perpendicular to $\hat{\mathbf{s}}_0$. Note that $\hat{\mathbf{y}}^S$ is equivalent to $\hat{\mathbf{y}}$ in the laboratory frame.

3 Interaction of electrons with the Gaussian beam

The interaction of electrons with the spatially localized Gaussian beam is given by the Lorentz equation,

$$\frac{d\mathbf{p}}{dt} \;=\; -e\,\left\{\mathbf{E}_{RF} \;+\; \frac{\mathbf{p}}{m_e\gamma}\;\times\;(\mathbf{B}_0 \;+\; \mathbf{B}_{RF})\right\} \qquad (7)$$

where $\mathbf{p}$ is the electron momentum, e is the magnitude of the electron charge, $\mathbf{B}_0$ is the uniform background magnetic field,

$$\gamma \;=\; \sqrt{1 \;+\; \frac{\mathbf{p}.\mathbf{p}}{(m_e c)^2}} \qquad (8)$$

and, m_e is the rest mass of the electron. The RF wave magnetic field $\mathbf{B}_{RF}$ is obtained from (2) by replacing $\tilde{\mathbf{e}}_n$ in the numerator by $\mathbf{n}\times\tilde{\mathbf{e}}_n/c$ – this follows from Faraday's law.

4 Numerical results and discussion

In order to illustrate the effect of a Gaussian beam on the dynamics of electrons interacting with it, we assume the following parameters. The wave frequency and the plasma density are assumed to be 170 GHz and 2×10^{20} m^{-3}, respectively. The local magnetic field is chosen to be such that the electron cyclotron frequency is slightly less than the wave frequency, i.e, $B_0 \approx 6.07$ T. The width of the Gaussian beam is set to $w = 12$ cm with $n_{0\parallel} = 0.2$ being the wave number parallel to the direction of the magnetic field. The perpendicular wave number $n_{0\perp}$ is determined from the local cold plasma dispersion relation. All these quantities are needed to define the wave vectors and the polarizations of the planar waves that make up the Gaussian beam. The ambient magnetic field is along the $\hat{\mathbf{z}}$ direction and the beam $\mathbf{n}_0$ lies in the $x-z$ plane. The normalization of the electron velocity is with respect to the thermal velocity – the temperature is taken to be 15 keV. The relation between the magnitudes of the velocity and the momentum is $u = p/(m_e c)$.

In the numerical runs that are displayed below, the initial x, y, and z components of the electron momentum are $p_x/p_T = p_y/p_T = 2.5$, and $p_z/p_T \equiv p_\parallel/p_T = 4$, respectively. Here p_T is the magnitude of the electron thermal momentum. The center of the coordinate system $x = y = z = 0$ lies on the axis of the Gaussian beam. Figures 1 and 2 show the normalized parallel and perpendicular speeds of an electron as it passes through a 1 MW beam with an ordinary mode polarization. The electron is initially located outside the beam at $z = -25$ cm and

is moving in the positive z direction. As the electron traverses the beam the effect of the planar waves that comprise the Gaussian beam is quite apparent. The electron oscillates in the potential of each plane wave as it moves along the z-direction. The parallel and perpendicular momenta change rapidly, but the electron exits the beam with the same momenta as when it entered the beam. However, this changes when the beam power is increased. Figures 3 and 4 illustrate the corresponding results when the beam power is increased to 10 MW. Inside the beam, the motion of the electron is not as oscillatory and coherent as it was for 1 MW of beam power. There is a lack of symmetry around the center of the beam that is evident in Figs. 1 and 2. The net result is that the electron has gained parallel and perpendicular speed by the time it exits the beam – the combined effect implying an increase in the plasma current.

The dynamics of electrons changes significantly if the beam has the polarization of the extraordinary EC wave. In Figs. 5 and 6, the normalized parallel and perpendicular components of the velocity are plotted as function of time for the extraordinary wave polarization. The other parameters are the same as in Figs. 1 and 2. The motion of the electron inside the beam is random and different from the oscillatory motion in Figs. 1 and 2. The increase in the two components of the velocity after the electron exits the beam is large, and we would expect the corresponding change in the current carried by the electron to be substantial. The changes are even more sizable when the beam power is 10 MW. Figures 7 and 8 illustrate these changes. Again, the electron behaves differently inside the beam than when the wave polarization corresponds to the ordinary EC wave.

Another interesting aspect of the nonlinear interaction of electrons with a Gaussian beam is the difference in the dynamics when the electrons enter the beam from different directions. This effect manifests itself as the beam is propagating obliquely with respect to the magnetic field. In Figs. 9 and 10, we plot the normalized components of the velocity when the initial location of the electron is at $z = 25$ cm and, initially, $p_\parallel/p_T = -4$. In other words, the electron enters the beam from the positive z side with its parallel speed directed along the $-\hat{\mathbf{z}}$ direction. Figure 9 shows the evolution $u_\parallel$ as a function of time. The electron enters the beam from the right – defined with respect to $z = 0$. Inside the beam, the parallel speed changes sign, i.e., the electron gets reflected, and exits the beam from the same side as it enters. This reflection is due to the nonlinear ponderomotive force caused by the spatial variation in the beam profile. The interaction of the electron with the beam is spatially restricted as it does not traverse through the entire width of the beam. This also limits the increase in the magnitude of the perpendicular velocity, as is evident when comparing Fig. 10 with Fig. 8.

The results displayed in Figs. 7 – 10 elucidate the importance of nonlinear effects in the interaction of electrons with a Gaussian beam. Let us define left and right with respect to the center of the beam at $z = 0$. Electron 1 entering the beam from the left transits through the beam and exits on the right with an increase in its velocity along

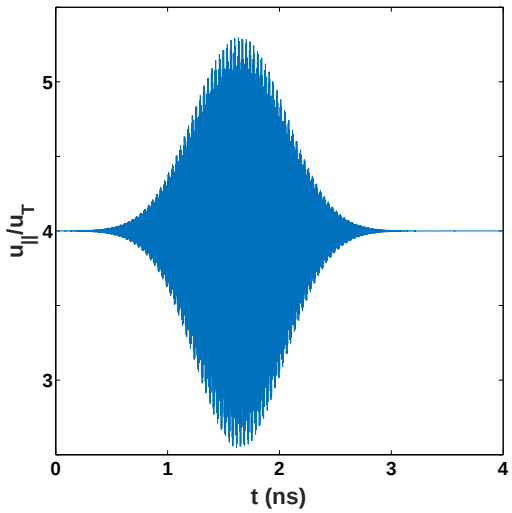

Figure 1. The evolution of $u_\parallel/u_T$ as a function of time. The initial position of the electron is outside the beam and it is moving along the positive z direction. The Gaussian beam has the polarization of the ordinary EC wave and power of 1MW. The other parameters are as indicated in the text.

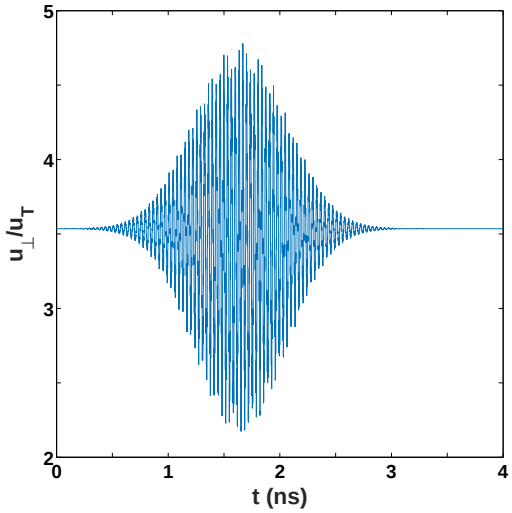

Figure 2. The evolution of $u_\perp/u_T$ as a function of time for the same parameters as in Fig. 1; $u_\perp/u_T = \sqrt{p_x^2 + p_y^2}/p_T$

the magnetic field line as well as gaining energy from the beam (Figs. 7 and 8). Electron 2 has the same initial energy and momentum as electron 1 except that its starting momentum parallel to the magnetic field is in a direction opposite to the starting parallel momentum of electron 1. Electron 2 is initially located to the right of the beam. During its transit through the beam, the parallel velocity reverses sign and the electron exits the beam from the same right side that it had entered the beam. The energy and the magnitude of the parallel velocity have increased relative to their initial values (Figs. 9 and 10). Electrons 1 and 2, which were initially traveling in opposite directions, are now moving in the same direction parallel to the magnetic

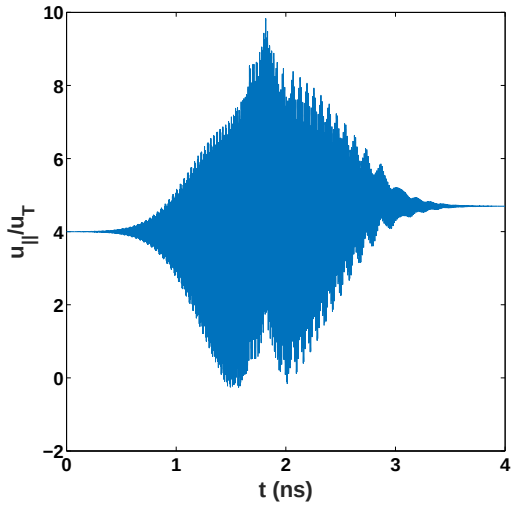

Figure 3. The parameters are the same as in Fig. 1 except that the beam power is 10 MW.

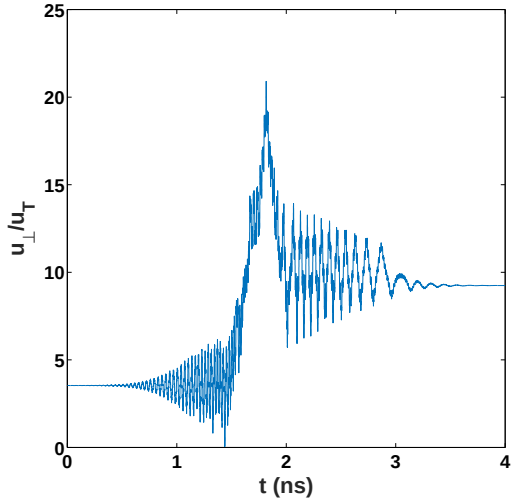

Figure 4. Same as Fig. 2 except that the beam power is 10 MW.

field. The practical consequence of this is an enhancement in the net plasma current.

5 Acknowledgement

AKR was supported by US DoE Grants DE-FG02-91ER54109 and DE-SC0018090.

References

[1] E. B. Hooper, et al., "MTX Final Report," [https://www.osti.gov/scitech/servlets/purl/10194124] (1994).
[2] M. Thumm, "State-of-the-Art of High Power Gyro-Devices and Free Electron Lasers," KIT Scientific Report 7735 (2016).
[3] W. M. Nevins, T. D. Rognlien, and B. I. Cohen, Physical Review Letters **59**, 60 (1987).
[4] D. Farina, Nuclear Fusion **58**, 066012 (2018).
[5] R. Kamendje, S. V. Kasilov, W. Kernbichler, and M. F. Heyn, Physics of Plasmas **10**, 75 (2003).
[6] R. Kamendje, S. V. Kasilov, W. Kernbichler, I. V. Pavlenko, E. Poli, and M. F. Heyn, Physics of Plasmas **12**, 012502 (2005).

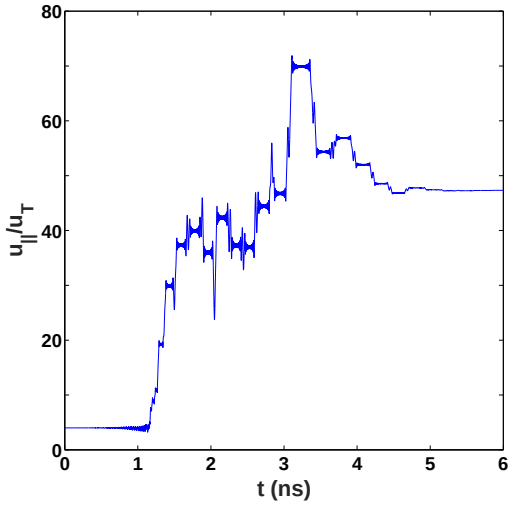

Figure 5. Same as Fig. 1 except that the beam polarization is of the extraordinary EC wave.

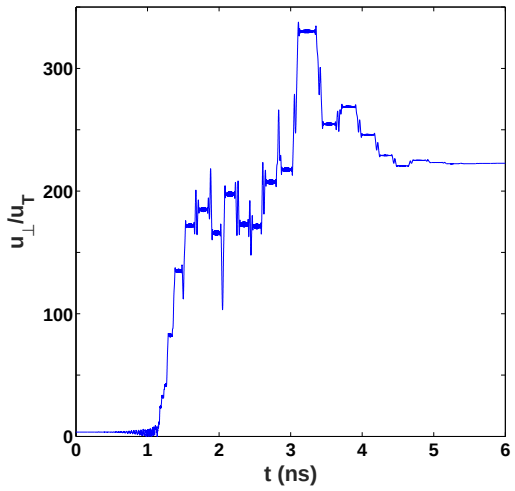

Figure 6. Same as Fig. 2 except that the beam polarization is of the extraordinary EC wave.

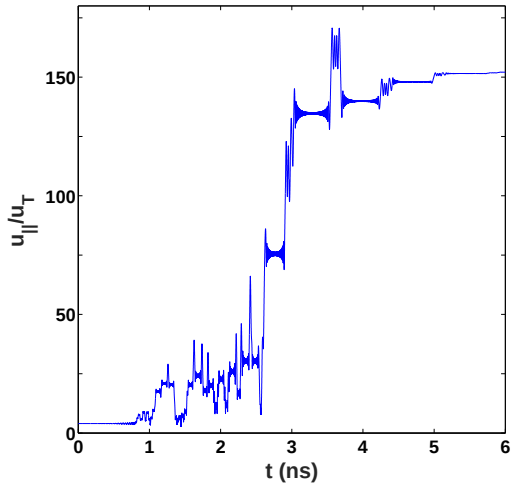

Figure 7. Same as Fig. 5 except that the beam power is 10 MW

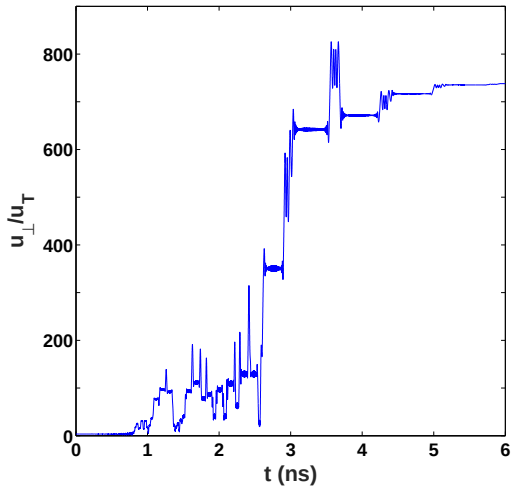

Figure 8. Same as Fig. 6 except that the beam power is 10 MW

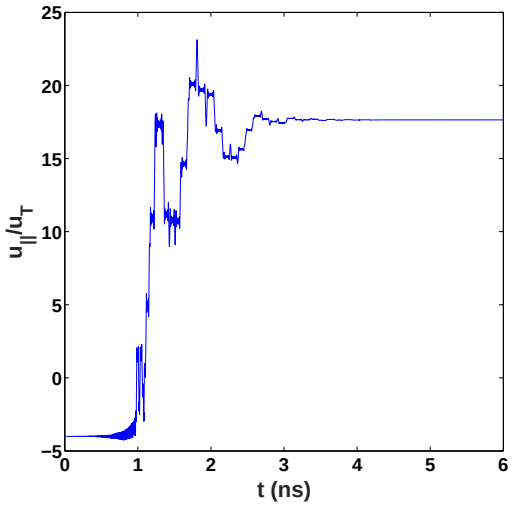

Figure 9. The beam polarization corresponds to the extraordinary EC wave and the beam power is 10 MW. The initial location and magnitude of the parallel velocity of the electron are $z = 25$ cm and $u_\parallel/u_T = -4$, respectively. All the other parameters are as described in the text.

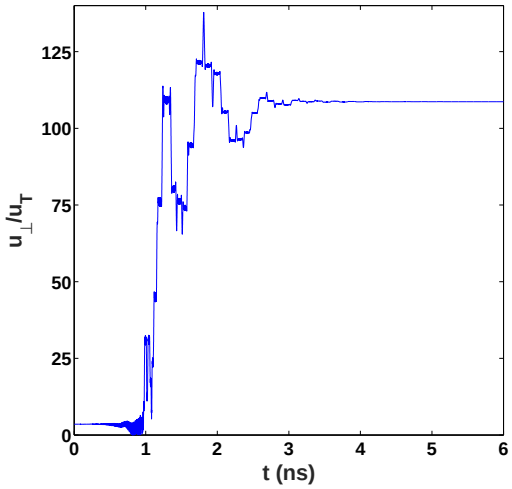

Figure 10. A plot of $u_\perp/u_T$ as a function of time for the same parameters as for Fig. 9.